

05

## Formation of periodic two-phase structures on the surface of amorphous $\text{Ge}_2\text{Sb}_2\text{Te}_5$ films under the action of ultrashort laser pulses of different durations and repetition rates

© M.P. Smayev<sup>1</sup>, P.I. Lazarenko<sup>2</sup>, M.E. Fedyanina<sup>2</sup>, I.A. Budagovsky<sup>1</sup>, A. Raab<sup>2</sup>, I.V. Sagunova<sup>2</sup>, S.A. Kozyukhin<sup>3,4</sup>

<sup>1</sup> Lebedev Physical Institute, Russian Academy of Sciences, 119991 Moscow, Russia

<sup>2</sup> National Research University of Electronic Technology, 124498 Zelenograd, Moscow, Russia

<sup>3</sup> Kurnakov Institute of General and Inorganic Chemistry, Russian Academy of Sciences, 119991 Moscow, Russia

<sup>4</sup> Tomsk State University, 634050 Tomsk, Russia

e-mail: smayev@lebedev.ru

Received December 20, 2022

Revised January 13, 2023

Accepted January 28, 2023

Phase change materials due to their high susceptibility to low-intensity light fields are extremely attractive for active microphotonics and integrated optics devices. As a result of fast phase switching, these materials change the refractive index in a wide spectral range, which has found application in information storage systems. In this work, we studied the formation of two-phase periodic structures consisting of alternating lines of amorphous and crystalline phases on the surface of thin-film  $\text{Ge}_2\text{Sb}_2\text{Te}_5$  phase change materials exposed to ultrashort laser pulses. Periodic structures were formed at a wavelength of 1030 nm at different durations and repetition rates of light pulses. It has been established that the development of two-phase structures obtained at a constant energy fluence remains practically unchanged with an increase in the repetition rate from 10 kHz to 1 MHz, but a change in the pulse duration from 180 fs to 10 ps leads to a violation of the periodic structure due to the formation of extended continuously crystallized regions.

**Keywords:** chalcogenide films,  $\text{Ge}_2\text{Sb}_2\text{Te}_5$ , phase change materials, laser-induced periodic surface structures, two-phase structures.

DOI: 10.61011/EOS.2023.02.55783.15-23

### Introduction

In the recent decades, phase change materials based on thin chalcogenide films have attracted high interest due to their unique physical and chemical properties [1–3]. This unique feature is primarily caused by fast (less than 100 ns [4,5]) reversible switching between the crystalline and amorphous phase states (up to 100 trillion cycles [6]), whose optical characteristics differ significantly [7]. Phase state switching may be induced by external pulses (thermal, electrical, optical, etc.).

The ternary compound  $\text{Ge}_2\text{Sb}_2\text{Te}_5$  (GST225) is the most distinguished and well-studied representative of phase change materials. It is widely used as a functional material to implement the controlled devices for nanophotonics, integrated optics, data storage and display [8–10]. Impact of low-power ultrashort (femtosecond and picosecond) laser pulses on thin amorphous GST225 films can, in addition to phase switching [11,12], lead to such structural effects as single-pulse crystallization [12,13], multistage crystallization [14,15], formation of binary (two-phase) laser-induced periodic surface structures (LIPSS) [16–19].

The latter are crystallized and amorphous lines alternating with a period close to the laser wavelength and oriented perpendicular to the light field polarization. This selective spatial crystallization may be explained by surface plasmon polariton formation and its interference with the incident radiation [17,18]. Nevertheless, many gaps still remain in understanding the mechanisms of phenomena that accompany the action of ultrashort pulses on thin films, therefore investigation of various laser exposure conditions is essential for solution of both fundamental and application tasks. Of particular interest is the identification of the parameters of laser irradiation leading to LIPSS formation due to the benefits of this approach for micro- and nanostructuring of chalcogenide semiconductor surfaces. Formation of periodic two-phase structures in a wide duration and repetition rate ranges of near infrared laser pulses was investigated herein.

### Materials and experimental technique

Amorphous GST225 thin films with a thickness of 130 nm were produced by DC magnetron sputtering of a polycrystalline target. Argon pressure during sputtering reached

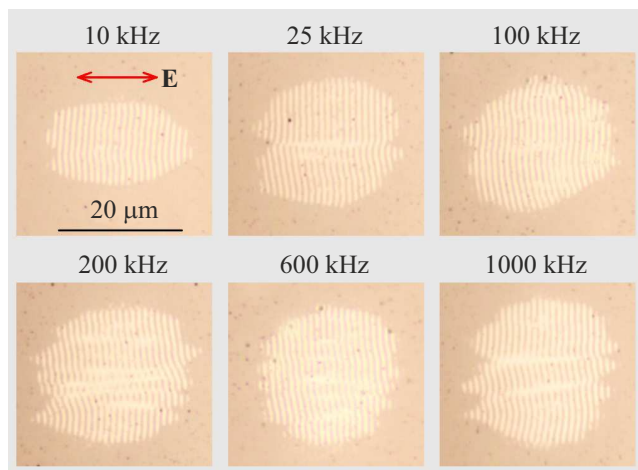


**Figure 1.** Optical microscopy images of regions containing periodic structures on the GST225 surface after the exposure to laser radiation with different femtosecond pulse repetition rates. Energy fluence is  $F = 2.6 \text{ mJ/cm}^2$ , the number of pulses is  $N = 2^{18}$ .  $\mathbf{E}$  is the laser beam polarization direction.

$5.6 \cdot 10^{-1} \text{ Pa}$ , and the power delivered to the target was 25 W. Two types of substrates with different thermal and optical properties were used. Both substrates were based on boron doped silicon wafers with a  $1 \mu\text{m}$  silicon oxide layer formed on the surface. For one type of substrates, 50 nm TiN and 200 nm W layers were additionally deposited by magnetron sputtering. The TiN layer served as an adhesive sublayer for tungsten which acted as a contact layer for GST225, because it meets the melting temperature, thermal stability and conductivity requirements. The types of substrates will be hereinafter referred to as „silicon“ and „metal“, respectively. Surface roughness, phase state and elemental composition distribution for as-deposited films were controlled by atomic-force microscopy, X-ray diffraction analysis and Auger electron spectroscopy methods.

Photoinduced surface modification was produced by 1030 nm Yb:KGW-based ultrashort laser pulse system. The repetition rate of light pulses  $f$  was controlled using an internal pulse picker; in the performed studies,  $f$  varied from 10 kHz to 1 MHz. Pulse length  $\tau$  was varied in the range from 180 fs to 10 ps using a built-in pulse compressor. The compressor was calibrated using PulseCheck (APE) autocorrelator. The radiation was linearly polarized and focused with a 75 mm lens (beam waist size  $w_0 = 25 \mu\text{m}$  by intensity level  $1/e^2$ ).

The sample was placed into a precision 3d positioner and exposed at film movement perpendicular to the optical axis. The sample displacement and laser emission parameters were controlled automatically, which made it possible to perform dot matrix recording on the surface of amorphous GST225 by varying the average power and the number of ultrashort pulses. The orientation homogeneity of the recorded two-phase periodic structures was assessed by the conventional pixel orientation dispersion (DLOA) [20]

for the LIPSS optical images. DLOA dispersion was determined using OrientationJ module in ImageJ image analysis software using the technique for quality assessment of laser-induced structures on metal surfaces [20,21].

## Results and discussion

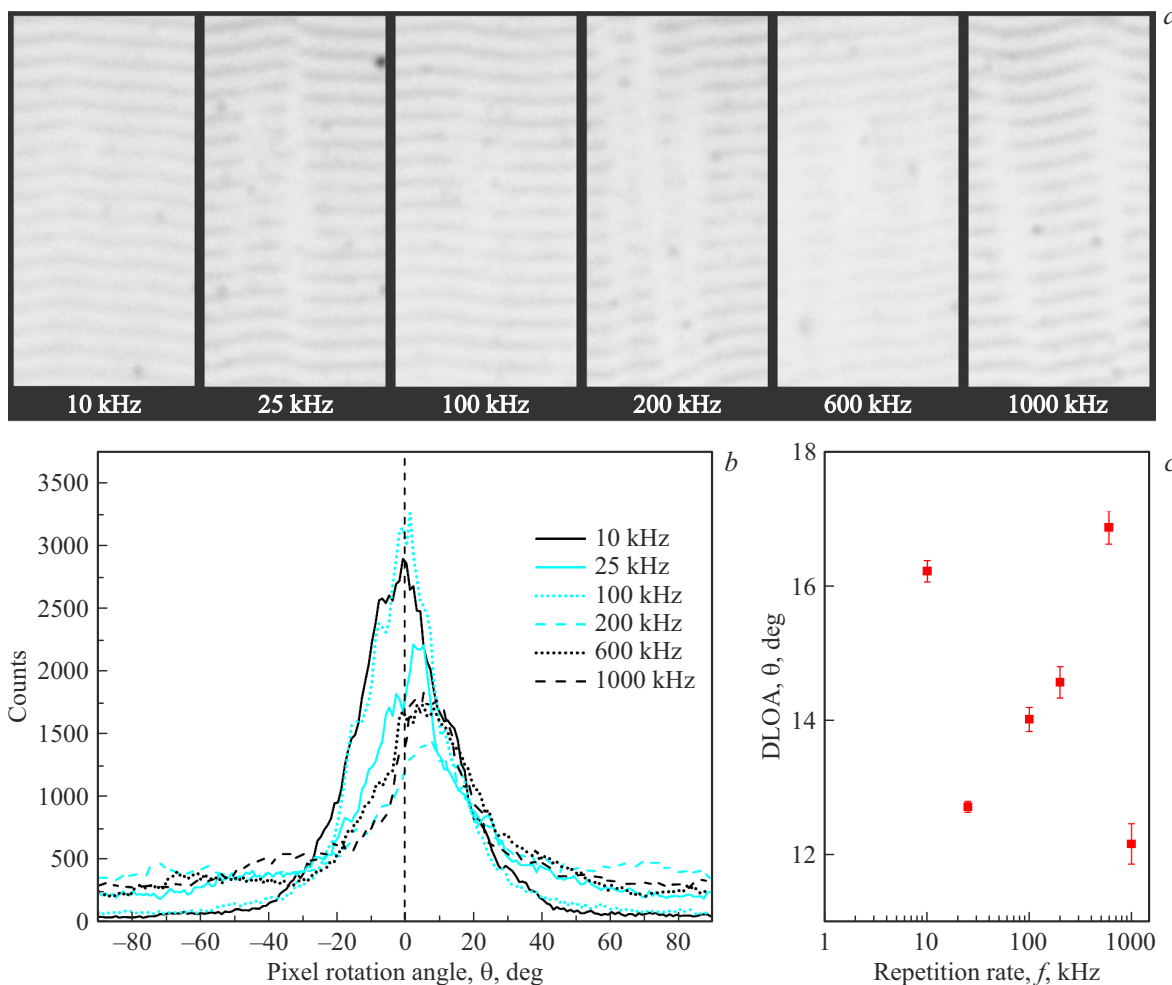
Depending on the exposure parameters, three types of regions were formed on the GST225 surface: (1) structures produced after film surface ablation and damage, (2) uniformly crystallized spots, (3) regions containing periodic two-phase structures (Figure 1, bright lines correspond to the crystalline phase, dark lines correspond to the amorphous phase). The purpose of the study was to investigate the periodic structure formation with various pulse radiation parameters. Periodic structures appear at rather low laser pulse energy fluences within  $F = 2.2\text{--}3.8 \text{ mJ/cm}^2$ , while at energy densities lower than  $2.2 \text{ mJ/cm}^2$ , there were no traces of laser exposure modification on GST225 surface, and at energy fluences higher than  $3.8 \text{ mJ/cm}^2$ , uniform surface crystallization prevailed. The period of the lines of the structure was approx  $1 \mu\text{m}$ , i.e., it correlated well with the exposure wavelength. The lines are oriented perpendicular to the light polarization vector. It should be noted that no periodic structures are formed in a low-pulse mode: the minimum number of pulses at which structured spots were observed was  $N_{\text{min}} = 256 (2^8)$  pulses, which is indicative of a kind of cumulative spot formation mode.

**Influence of femtosecond pulse repetition rate.** To study the laser frequency influence, a metal substrate sample was used. Pulse length was  $\tau = 180 \text{ fs}$ . The sample was moved from the focal plane by  $\Delta = 1.2 \text{ mm}$ , in this case, the spot diameter on the sample surface was about  $70 \mu\text{m}$ . According to [19], such small displacement into a diverging beam causes more uniform intensity profile which is favorable for achievement of regions filled with regular two-phase periodic structures.

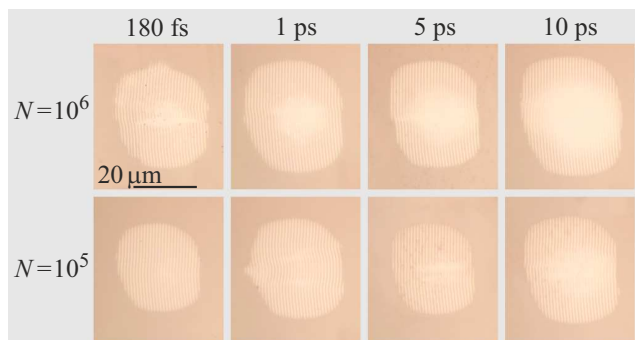
To assess the impact of pulse repetition rate  $f$ , we recorded several dot series with the same pulse energy (and different average power). The pulse repetition rate  $f$  was varied from 10 kHz to 1 MHz.

Figure 1 shows the structured spot images obtained at various repetition rates  $f$ , energy fluence  $F = 2.6 \text{ mJ/cm}^2$  and number of pulses  $N = 2^{18} = 262144$ . It can be seen that, the character of film modification varies insignificantly throughout the frequency range (10 kHz–1000 kHz), despite the fact that the mean power of the recording emission increases by two orders with such frequency growth. This suggests that formation of spots filled with periodic surface structures depends on the pulse energy, rather than on the repetition rate.

For regions modified at various  $f$  (Figure 1), DLOA analysis of central parts was carried out (Figure 2, a), which showed a fairly consistent overall orientation of the periodic structures: angular distribution peak positions



**Figure 2.** Conventional pixel orientation dispersion analysis (DLOA analysis) of two-phase structures obtained during exposure of GST225 thin films to ultrashort pulses with different repetition rates  $f$ . *a* — images of central parts of modified regions (selected from Figure 1) used quantitative assessment of LIPSS ordering; *b* — angular pixel orientation distribution in the selected regions; *c* — dependence of pixel orientation dispersion vs. pulse repetition rate.



**Figure 3.** Optical microscopy of periodic structures formed on GST225 surface on the silicon substrate after exposure to  $10^6$  and  $10^5$  laser pulse series with different pulse lengths. Energy fluence is  $F = 3.5 \text{ mJ/cm}^2$ .

differ no more than  $5^\circ$  (Figure 2, *b*). Dependence of dispersion  $\theta$  on the pulse repetition rate is not mono-

tonic (Figure 2, *c*) and is apparently associated with local phase state heterogeneities distorting the LIPSS shape. It should be noted that in accordance with the conclusion in [21], the presence of defects (in our case — uniform crystallization zones in the center of the selected regions) has a little effect on the magnitude of dispersion, which helps to assess the orientation uniformity of two-phase structures.

**The influence of pulse lengths.** Experimental investigations of pulse length influence were carried out for samples on silicon and metal substrates. The pulse repetition rate was constant  $f = 200 \text{ kHz}$ . The sample was placed at  $\Delta = 1.4 \text{ mm}$  from the focal plane of the lens, in this case, the spot diameter on the sample surface was  $2w = 80 \mu\text{m}$ . For both substrates with length  $\tau$  increased from 180 fs to 10 ps and the same number of pulses, no significant spot shape variation takes place, however, appearance and increase of the inner crystalline region (Figure 3) is apparent and is caused by the increased exposure time during one

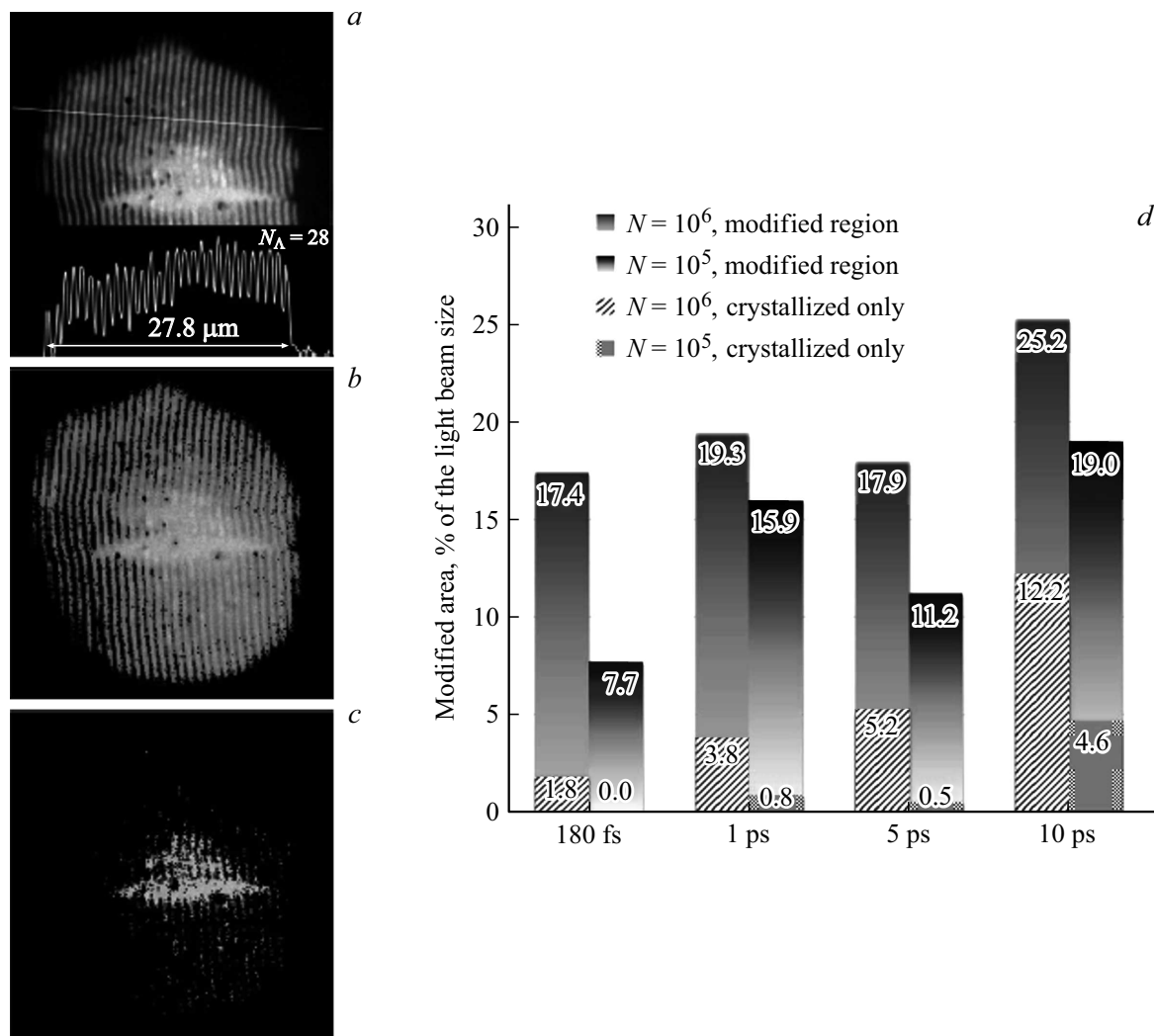


**Figure 4.** Image processing stages to determine the ratio of modified regions and continuous crystallization regions on the example of the first frame of Figure 3, *a* ( $\tau = 180$  fs,  $N = 10^6$ ): *a* — subtraction of the average background, *b* — selection of the modification region using binarization by color components  $R > 25$ ,  $G > 25$ ,  $B > 25$ , *c* — selection of the crystallization region using binarization by color components  $R > 25$ ,  $G > 45$ ,  $B > 45$ . Diagram of the ratio of the areas of modified or crystallized regions to the area of the light beam for various laser pulse lengths (*d*).

pulse. At  $N = 10^6$  and pulse lengths higher than 1 ps, LIPSS zone occupies a smaller portion of the modified region (Figure 3); in this cases, comparative assessment of the conventional pixel orientation is hindered. Dimensions of the modification and uniform crystallization regions vs. the light beam size may be used here as a quantitative parameter. For simple assessment of these parameters, we used image filtration by RGB component levels after subtraction of the average background determined by a non-modified region on the beam periphery (Figure 4, *a*). Subsequent binarization by  $R > 25$ ,  $G > 25$ ,  $B > 25$  above the background level allowed to distinguish the modification region (Figure 4, *b*), while binarization by levels  $R > 25$ ,  $G > 45$ ,  $B > 45$  allowed to distinguish the continuous crystallization region (Figure 4, *c*). The number of non-zero pixels after binarization vs. the number of pixels

corresponding to the beam size is shown in Figure 4, *d*. It can be seen that for  $N = 10^5$ , the relative area of full crystallization zones is much lower than for  $N = 10^6$ , i.e. to achieve a modified region filled with regular LIPSS, approaches with fewer number of pulses should be used (Figure 3, lower row).

Optical image with subtracted background was used to determine the period of recorded structure by the intensity profile along the section line. For the line in Figure 4, *a*, the period  $\Lambda = 0.99 \mu\text{m}$  was obtained.

It should be noted that the most uniform filling of the exposed region with periodic structures occurs at the lowest laser pulse length (180 fs) used herein. This indicates the possibility of initiation of LIPSS formation on the surface of amorphous  $\text{Ge}_2\text{Sb}_2\text{Te}_5$  films by laser pulses with shorter length compared with typical laser crystallization time [5].

In general, formation of laser-induced periodic structures on the surface of thin  $\text{Ge}_2\text{Sb}_2\text{Te}_5$  films is observed in a rather wide pulse repetition rate and length range to enable flexible selection of equipment to form LIPSS within a certain task due to the point optimization of laser exposure conditions.

## Conclusions

Formation of two-phase periodic surface structures after laser pulse exposure was investigated. It has been found that LIPSS formation under exposure to pulses with a wavelength of 1030 nm took place in a rather narrow low-energy laser exposure mode (energy fluence  $F = 2.2\text{--}3.8\text{ mJ/cm}^2$ ), but in a wide light pulse length range 180 fs ÷ 10 ps and at pulse repetition rates from 10 kHz to 1 MHz.

It has been found that, at constant energy density, the form of a spot containing the alternating amorphous and crystalline phase lines is almost independent of the type of substrate, repetition rate or pulse length, however, the increase in pulse length causes increase in the internal continuously crystallized region due to the exposure time increase. Such behavior may be associated with the features of heat transfer during one pulse.

## Funding

Material synthesis, film formation and characterization were covered by a grant of the Russian Science Foundation No. 18-79-10231. LIPSS were produced and studied in the research laboratory „Active Photonics Materials and Devices“ under the sponsorship of the Ministry of Science and Higher Education of the Russian Federation (Agreement No. 075-03-2022-212/4 from 08.11.2022, FSMR-2022-0001).

## Conflict of interest

The authors declare that they have no conflict of interest.

## References

- [1] C. Wu, H. Yu, S. Lee, R. Peng, I. Takeuchi, M. Li. *Nature Commun.*, **12** (1), 96 (2021). DOI: 10.1038/s41467-020-20365-z
- [2] M. Xu, X. Mai, J. Lin, W. Zhang, Y. Li, Y. He, H. Tong, X. Hou, P. Zhou, X. Miao. *Adv. Funct. Mat.*, **30**, 2003419 (2020). DOI: 10.1002/adfm.202003419
- [3] S.A. Kozyukhin, P.I. Lazarenko, A.I. Popov, I.L. Eremanko. *Russ. Chem. Rev.*, **91** (9), RCR5033 (2022). DOI: 10.1070/RCR5033.
- [4] D. Loke, T.H. Lee, W.J. Wang, L.P. Shi, R. Zhao, Y.C. Yeo, T.C. Chong, S.R. Elliott. *Science*, **336**, 1566 (2012). DOI: 10.1126/science.1221561
- [5] A.V. Kiselev, V.V. Ionin, A.A. Burtsev, N.N. Eliseev, V.A. Mikhalevsky, N.A. Arkharova, D.N. Khmelenin, A.A. Lotin. *Opt. Laser Technol.*, **147**, 107701 (2022). DOI: 10.1016/j.optlastec.2021.107701
- [6] I.S. Kim, S.L. Cho, D.H. Im, E.H. Cho, D.H. Kim, G.H. Oh, D.H. Ahn, S.O. Park, S.W. Nam, J.T. Moon, C.H. Chung. *2010 Symposium on VLSI Technology* (IEEE, 2010), p. 203. DOI: 10.1109/VLSIT.2010.5556228
- [7] A.A. Burtsev, N.N. Eliseev, V.A. Mikhalevsky, A.V. Kiselev, V.V. Ionin, V.V. Grebenev, D.N. Karimov, A.A. Lotin. *Mat. Sci. Semicon. Proc.*, **150**, 106907 (2022). DOI: 10.1016/j.mssp.2022.106907
- [8] P. Guo, A.M. Sarangan, I. Agha. *Appl. Sci.*, **9** (3), 530 (2019). DOI: 10.3390/app9030530
- [9] P. Lazarenko, V. Kovalyuk, P. An, A. Prokhodtsov, A. Golikov, A. Sherchenkov, S. Kozyukhin, I. Fradkin, G. Chulkova, G. Goltsman. *APL Mater.*, **9**, 121104 (2021). DOI: 10.1063/5.0066387
- [10] C.Y. Hwang, G.H. Kim, J.H. Yang, C.S. Hwang, S.M. Cho, W.J. Lee, J.E. Pi, J.H. Choi, K. Choi, H.O. Kim, S.Y. Lee, Y.H. Kim. *Nanoscale*, **10** (46), 21648 (2018). DOI: 10.1039/C8NR04471F
- [11] G. Zhang, D. Gu, F. Gan, X. Jiang, Q. Chen. *Thin Solid Films*, **474**, 169 (2005). DOI: 10.1016/j.tsf.2004.08.122
- [12] X. Sun, M. Ehrhardt, A. Lotnyk, P. Lorenz, E. Thelander, J.W. Gerlach, T. Smausz, U. Decker, B. Rauschenbach. *Sci. Rep.*, **6**, 28246 (2016). DOI: 10.1038/srep28246
- [13] T. Kunkel, Yu. Vorobyov, M. Smayev, P. Lazarenko, A. Romashkin, S. Kozyukhin. *Mat. Sci. Semicon. Proc.*, **139**, 106350 (2022). DOI: 10.1016/j.mssp.2021.106350
- [14] T. Kunkel, Yu. Vorobyov, M. Smayev, P. Lazarenko, V. Veretennikov, V. Sigaev, S. Kozyukhin. *J. Alloy. Compd.*, **851**, 156924 (2021). DOI: 10.1016/j.jallcom.2020.156924
- [15] S. Wen, Y. Meng, M. Jiang, Y. Wang. *Sci. Rep.*, **8**, 4979 (2018). DOI: 10.1038/s41598-018-23360-z
- [16] S.A. Yakovlev, A.V. Ankudinov, Y.V. Vorobyov, M.M. Voronov, S.A. Kozyukhin, B.T. Melekh, A.B. Pevtsov. *Semiconductors*, **52** (6), 809 (2018). DOI: 10.1134/S1063782618060246.
- [17] S. Kozyukhin, M. Smayev, V. Sigaev, Yu. Vorobyov, Yu. Zaytseva, A. Sherchenkov, P. Lazarenko. *Phys. Status Solidi B*, **257**, 1900617 (2020). DOI: 10.1002/pssb.201900617
- [18] S. Zaboltnov, A. Kolchin, D. Shuleiko, D. Presnov, T. Kaminskaya, P. Lazarenko, V. Glukhenkaya, T. Kunkel, S. Kozyukhin, P. Kashkarov. *Micro*, **2**, 88 (2022). DOI: 10.3390/micro2010005
- [19] M.P. Smayev, P.I. Lazarenko, I.A. Budagovsky, A.O. Yakubov, V.N. Borisov, Y.V. Vorobyov, T.S. Kunkel, S.A. Kozyukhin. *Opt. Laser Technol.*, **153**, 108212 (2022). DOI: 10.1016/j.optlastec.2022.108212
- [20] I. Gnilitzkyi, T.J. Derrien, Y. Levy, N.M. Bulgakova, T. Mocek, L. Orazi. *Sci. Rep.*, **7**, 8485 (2017). DOI: 10.1038/s41598-017-08788-z
- [21] D.A. Belousov, A.V. Dostovalov, V.P. Korolkov, S.L. Mikerin. *Komp'yuternaya optika*, **43** (6), 936 (2019) (in Russian). DOI: 10.18287/2412-6179-2019-43-6-936-945

Translated by E.Ilyinskaya